JETIR.ORG ISSN: 2349-5162 | ESTD Year : 2014 | Monthly Issue
JOURNAL OF EMERGING TECHNOLOGIES AND INNOVATIVE RESEARCH (JETIR)
An International Scholarly Open Access, Peer-reviewed, Refereed Journal

Multi-scale Exposure Fusion for Low Dynamic Range Images

[1]Mr. NeerugantiVikramTeja, [2]P Vamsi, [3]Ms. Neelima K. [4]Nune Divya,

[1,3,4]Assistant Professor,[2]M Tech scholar
[1]vikramtejan@gmail.com, [2]vamsikarthick436@gmail.com, [3]neelumtech17@gmail.com, [4]divyapsdv1995@gmail.com
[1,2,3,4]Department of Electronics and Communication Engineering,
[1,3,4]Sree Vidyanikethan Engineering College, Tirupati,India.[2]IIT, Kanpur, India.

Abstract : This paper projects a new multi-scale exposure fusion algorithm to merge differently exposed low dynamic range (LDR) images by using the weighted guided image filter (WGIF) to smooth the Gaussian pyramids of weight maps. In the fused image, the details in the brightest and darkest regions of the HDR scene are preserved better without any change in relative brightness. Also a new weighted structure tensor is considered to the differently exposed images for enhanced detail extraction according to the preference. The proposed multi-scale exposure fusion algorithm with filter is suitable for a simple single image brightening algorithm for both low-light imaging and back-light imaging. The proposed algorithm yields better images for human perception. The results are compared for various parameters and the proposed design is found to be a better choice of processing the Multi-Scale Exposure images fusion due to better parameter values of standard deviation and entropy.

Index Terms **- Dynamic Range, Entropy, Gaussian Pyramids, Multi-scale exposure fusion, Weight Maps.**

I. INTRODUCTION

The image processing algorithms include various segmentation algorithms for low contrast images especially for early detection of abnormalities to help patients [1][2][3][4]. Identification of malignant nodules from the medical image is a critical task as the image may contain noise during the processing that can be unseen and also having similar intensities of unwanted tissue thickening [5][6]. The image dynamic range reflects the persons' mental stability which might get affected and may further lead to chronic ailments due to persistent stress [7]. Denoising of images can be performed with suitable regularization terms by using non-local similarity features to improve the quality of reconstructed images [8].

The hybrid decomposition to obtain high-quality tone mapped image [9] use edge-preserving and structural priors to remove the halo effects while preserving useful edges. The tools for integration of segmentation, extraction and classification of image scan are developed such as Hospital Information System (HIS) and Picture Archiving and Communication Systems (PACS) using digital entities to maintain medical examinations, images and statements [10]. Other techniques like Support Vector Machine [11], Convolutional neural networks (CNNs) [12][13], Artificial Intelligence [14] for feature extraction and classification [15][16][17][18].

With the latest developments like improved robustness and increased resolution of modern imaging sensors, cheaper fabrication cost enabled the use of multiple sensors common in a wide range of imaging applications. However, the subsequent processing of the gathered multi sensor information can be cumbersome since an increase in the number of sensors automatically leads to an increase in the raw amount of sensor data which needs to be stored and processed. This requires longer execution times or large computation costs i.e., the number of processing units and storage devices. In addition to these, images taken by human present overwhelming task for a single observer and may lead to a significant performance drop. By using a single composite representation which incorporates all relevant sensor data proves to be a better solution, called as image fusion [19].

Image fusion is the non trivial process of integrating complementary and redundant information from multiple images into one composite image that contains a 'better' description of the underlying scene than any of the individual source images could provide. As fusion uses the source images taken from different types of sensors having different dynamic range and resolution, the features extracted tend to exhibit complementary information or they may have a common information but with reversed contrast, which significantly complicates the fusion process.

Also as fusion approach is independent of a priori information about the inputs and produces a composite image that appears 'natural' to a human interpreter is highly desirable. The basic requirements of fusion algorithms are all relevant information in input images must be preserved, it should not introduce any artifacts or inconsistencies which can distract or mislead a human observer or any subsequent image processing task and it should be reliable, robust and tolerant of imperfections such as noise and misregistrations.

The fusion algorithms may be applied to images taken from different sensors (multisensor fusion), taken at different times (multitemporal fusion), obtained using various focal lengths (multifocus fusion), taken from different viewpoints (multiview fusion) or captured under different exposure settings (multiexposure fusion). The application areas include military, remote sensing, medical science, industrial engineering, etc.

II. EXISTING TECHNIQUES

Image fusion techniques blend information present in different images into a single image [20]. In recent years, various fusion algorithms have been developed to combine substantial information from multiple input images into a single composite image.

The principal motivation for image fusion is to extend the DOF, extend spatial and temporal coverage, to increase reliability, extend DR of the fused image and the compact representation of information. Imaging sensor records the time and space varying light intensity information reflected and emitted from object in a three-dimensional observed physical scene. However, the characteristics recorded from the incident radiations in the source images, such as exposure value, focusing, modality, and environmental conditions, often make fusion extremely challenging [21].

The automated procedure of extracting all the meaningful details from the input images to a final fused image is the main motive of image fusion [22]. To facilitate image fusion, it may be necessary to align input images of the same scene captured at different times, or with different sensors, or with EV settings (called AEB), or from different viewpoint using local and global registration methods [23].

Normally it is assumed that the input images are captured with the help of tripod mounting. Hence, in general, image fusion approach expects point-by-point correspondence between different input exposures of a scene. From technical stand point, the fused image reveals all details present in the scene without introducing any artifacts or inconsistencies which would distract the human observer or subsequent image processing stages [24]. The Laplacian pyramid representation expresses an image as a sum of spatially band-passed images while retaining local spatial information in each band [25].

Another multi-resolution based fusion which employs gradient map of the input images to yield a fused image with true information [26]. This approach takes into account the horizontal and vertical gradient maps for producing fused gradient map for each orientation and resolution [27]. This gradient fusion approach utilizes Discrete Wavelet Transform (DWT) and Quadrature Mirror Filters (QMFs) in the reconstruction process. This approach was implemented for input data provided by multi-sensory arrays. Another multi-sensor data fusion technique which utilizes Total Variation (TV).

In pixel-level approach, the TV semi-norm is used to solve the forward model and estimate the pixels of the fused. The input data set used in this approach is taken from Computed Tomography (CT) and Magnetic Resonance Imaging (MRI). Moreover, this algorithm was also applied to visible-band and infrared sensors as well as the aircraft navigation images. Image gradient orientation coherence model based fusion [28] provides the solution to handle strong highlights and remove self-reflections from flash and ambient images. This model seeks to utilize the properties of image gradients that remain invariant under the change of lighting that takes place between a flash and an ambient image.

The support value computed from Mapped Least Squares Support Vector Machine (MLS-SVM) can be used as an indicator of salient features of image, which could be used for multi-sensory data fusion [29]. SVM is a recently proposed powerful tool for data classification and function estimation, and can be used for a variety of applications in image processing. This approach is based on the fact that, in SVMs [30], the data with larger support values have a physical meaning in the sense that they reveal relative more importance of the data points for contributing to the SVM model. In practice, in this approach, the SVM is used as multi-resolution transform, which directly provides the salient features of source image.

After decomposing input images into the sequence of support value images and the low-frequency components, choose-max method is used to select salient features in the fused image. This approach was developed for multi-focus and multi-sensor image fusion.

III. DETAIL ENHANCED FUSION

A new multi-scale exposure fusion algorithm is first proposed using the WGIF in [28]. A fast detail extraction algorithm is then proposed to enhance the proposed multi-scale exposure fusion algorithm. The three quality measures $C_i(p)$, $S_i(p)$, and $E_i(p)$ measure contrast, color saturation, and well exposedness of pixel $Z_i(p)$, respectively. The contrast, $C_i(p)$ is obtained by applying a Laplacian filter to the gray-scale version of each image. The color saturation, $S_i(p)$ is computed as the standard deviation within the R, G and B channel. The well exposedness, $E_i(p)$ is obtained by applying a

Gauss curve to each channel separately and multiplying the results. Their product is denoted as $W_i(p)$. The weight map is then constructed as

$$W_i(p) = \frac{\widehat{W}_i(p)}{\sum_{j=1}^{N} \widehat{W}_j(p)} \quad (1)$$

$G_f Y_i g(l)$ and $G_f W_i g(l)$ are the Gaussian pyramids of luminance component Y_i and weight map W_i, respectively.

The WGIF based pyramid is then given as

$$\{\widehat{w}_i\}^{(l)} = \{\hat{a}_i\}^{(i)}\{Y_i\}^{(l)} + \{\hat{b}_i\}^{(l)}; 1 \le l \le k \quad (2)$$

Let $L\{Z_{i,j}\}$ (l) be the Laplacian pyramid of component $Z_{i,j}$. All the images $Z_i(1 \le i \le N)$ at the different pyramid levels are blended as

$$L\{Z_j^{int}\}^{(l)} = \sum_{i=1}^{N} \left[L\{Z_{i,j}\}^{(l)}\{W_i\}^{(l)}\right]; j \in \{r, g, b\} \quad (3)$$

and the Laplacian pyramid $L\{Z_j^{int}\}$ (l) is collapsed to produce the intermediate image Z_j^{int}. The complexity of the proposed exposure fusion algorithm is O(NM) for N differently exposed images with M pixels.

The luminance components of the LDR images $Z_i(1 \le i \le N)$ and the intermediate image Z_{int} in log domain are computed as

$$\hat{Y}_i(p) = \log(Y_i(p) + 1)\ ;\ \hat{Y}^{int}(p) = \log(Y^{int}(p) + 1) \quad (4)$$

The two weights $\hat{W}_{x,i}(p)$ and $\hat{W}_{y,i}(p)$ are defined as

$$\hat{W}_{x,i}(p) = \frac{f(Y_i(p))f(Y_i(p_r))}{\max_j\{f(Y_j(p))f(Y_j(p_r))\}} \quad (5)$$

$$\hat{W}_{y,i}(p) = \frac{f(Y_i(p))f(Y_i(p_b))}{\max_j\{f(Y_j(p))f(Y_j(p_b))\}} \quad (6)$$

where p_r and p_b are the right and bottom pixels of the pixel p, and f(z) is defined as

$$f(z) = \begin{cases} z+1; & \text{if } z \le 128 \\ 257 - z; & \text{otherwise} \end{cases} \quad (7)$$

The weighted gradients of all the LDR images $Z_i(1 \le i \le N)$ at the pixel p are then given by the following matrix:

$$\nabla\hat{Y}(p) = \begin{bmatrix} \hat{W}_{x,1}(p)\frac{\partial\hat{Y}_1(p)}{\partial x} & \hat{W}_{y,1}(p)\frac{\partial\hat{Y}_1(p)}{\partial y} \\ \vdots & \vdots \\ \hat{W}_{x,N}(p)\frac{\partial\hat{Y}_N(p)}{\partial x} & \hat{W}_{y,N}(p)\frac{\partial\hat{Y}_N(p)}{\partial y} \end{bmatrix} \quad (8)$$

The weights of pixels of different source images are first estimated, and then refined by recursive filtering with the corresponding source image serving as the reference image. Finally, the fused image is constructed by weighted sum of source images.

When fusing images in static scenes without motion objects, two image features i.e., local contrast and brightness should be considered for weight estimation. The local contrast of each pixel is calculated as follows:

$$A_n = \widehat{I_n}(x, y) * h(x, y) \quad (9)$$

When fusing images in dynamic scenes which contain motion objects, as well as the local contrast and brightness feature, the influence of motion objects should also be considered for weight estimation. Through measuring the color dissimilarity between pixels of source images and pixels of the scene's static background, a novel histogram equalization and median filter based motion detection method is proposed. The temporal median filter has been widely used for motion. detection in video applications. It is based on the assumption that motion objects usually appear less times than pixels from the static background. Here, the temporal median filter is used to obtain the scene's static background image so that the motion objects of each image can be easily detected by calculating the color dissimilarity between each histogram equalized image and the scene's static background image.

In order to preserve image details and remove influences of under-exposed pixels, over-exposed pixels, and pixels from motion objects, the three image features i.e., local contrast, brightness, and color dissimilarity should be combined

together for weight estimation. The straightforward way to this objective is by multiplication. However, the pixels of the same location of different LDR images may be all labeled as under-exposed, over-exposed or motion objects, and this is unreasonable especially when these pixels appear in a large number. To solve this problem, the brightness feature and color dissimilarity feature are first combined together by multiplication:

The weights estimated above are noisy and hard (most weights are either 0 or 1). So the weight maps should be refined for weighted sum based image fusion. This is possible due to the recently proposed recursive filter [14], which is a real-time edge-preserving smoothing filter. Here, recursive filtering is performed on the weight maps ˆWn with the corresponding source image n I serving as the reference image.

$$W_n = R(\widehat{w_n}, I_n) \quad (10)$$

where R denotes the recursive filtering operation.

The weight map refinement step with recursive filter is based on two simple assumptions: first, pixels from the same objects which have similar image color should have similar weights; second, smooth weights are preferred since it will not introduce seam artifacts in the resulting fused image. Furthermore, to reduce the computing and memory consumption, all the weight maps can be computed at a half resolution of the original image size and then up-sampled to the original size for image fusion. This acceleration scheme has little influence to the performance of the proposed method.

IV. RESULTS AND DISCUSSION

The algorithms are compared using two parameters i.e., Entropy and Standard Deviation. The entropy (E) is defined as the measure of the overall information content of the given signal or data. It uses the probability density function of the signal in order to measure its randomness. High entropy denotes high randomness, and it shows that the information content of the signal is rich. In image fusion, entropy is used to measure the salient features in the fused image. The larger entropy means that the fused image contains more information and implies better image fusion. The formulation of E is given by

$$E = -\sum_{z=0}^{L} h_{I_f}(z) \log_2 h_{I_f}(z) \quad (11)$$

The Standard Deviation (SD) considers the histogram of the fused image and evaluates the fused image with respect to the width of its histogram. In image fusion, a larger SD means better image fusion. The formulation of SD is given by

$$SD = \sqrt{\sum_{z=0}^{L} (Z - \bar{Z})^2 h_{I_f}(z)} \quad (12)$$

where

$$\bar{Z} = \sum_{Z=0}^{L} Z h_{I_f}(z) \quad (13)$$

Where $h_{I_f}(z)$ is the normalized histogram of the fused image, If(x,y), and L is the number of bins in the histogram.

Figure 1 shows the input images of Tree Scenary with varying brightness as a series of seven images.

Figure 1: Input Images of Tree Scenary

Figure 2 shows the input images of Garage with varying brightness as a series of six images.

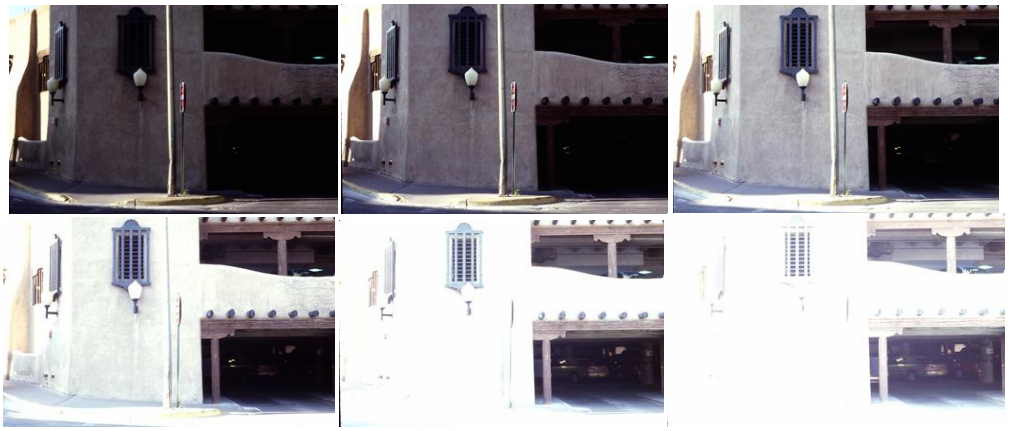

Figure 2: Input Images of Garage

Figure 3 shows the input images of Forest Sequence with varying brightness as a series of four images.

Figure 3: Input Images of Forrest Sequence

Figure 4 shows the processed images of Tree Scenary with and without contrast enhancement by using varied brightness for a series of seven images. and Multi-Scale Exposure Fusion Algorithm.

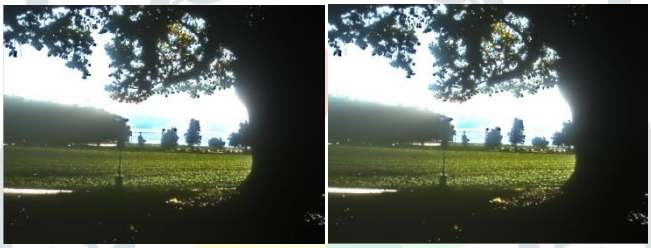

Figure 4: Multi-Scale Exposure of Tree Scenary without and with contrast enhancement

Figure 5 shows the processed images of Garage with and without contrast enhancement by using varied brightness for a series of six images. and Multi-Scale Exposure Fusion Algorithm.

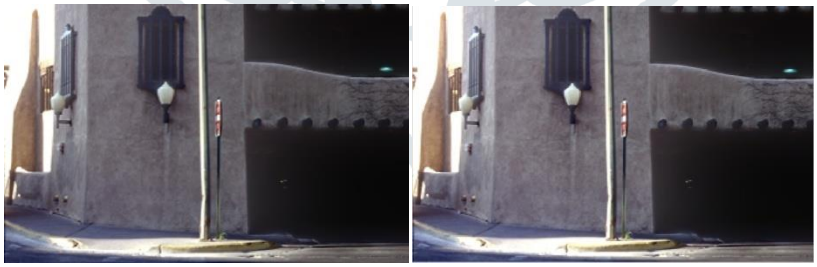

Figure 5: Multi-Scale Exposure of Garage without and with contrast enhancement

Figure 6 shows the processed images of Forest Sequence with and without contrast enhancement by using varied brightness for a series of four images. and Multi-Scale Exposure Fusion Algorithm.

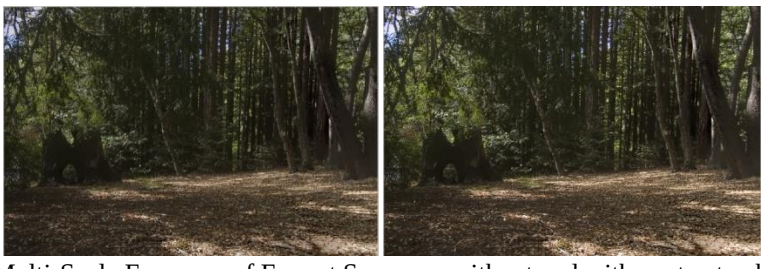

Figure 6: Multi-Scale Exposure of Forrest Sequence without and with contrast enhancement

Figure 7 shows the processed images of Tree scenary with and without contrast enhancement by using varied brightness for a series of seven images and Fast Multi-Scale Exposure Fusion using Median and Recursive Filters Algorithm.

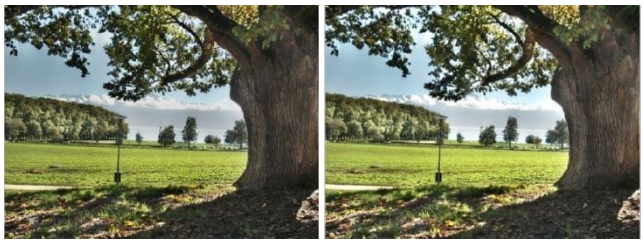

Figure 7: FMMR of Tree Scenary without and with contrast enhancement

Figure 8 shows the processed images of Garage with and without contrast enhancement by using varied brightness for a series of seven images and Fast Multi-Scale Exposure Fusion using Median and Recursive Filters Algorithm.

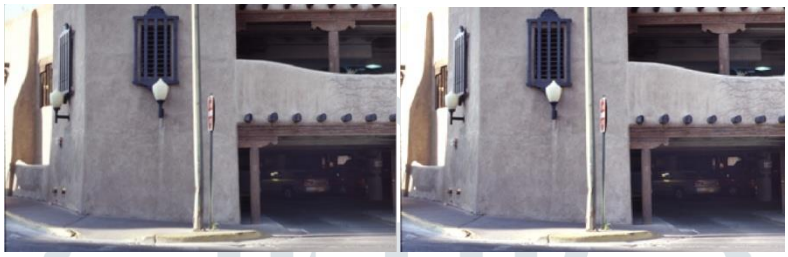

Figure 8: FMMR of Garage without and with contrast enhancement

Figure 9 shows the processed images of Forrest Sequence with and without contrast enhancement by using varied brightness for a series of seven images and Fast Multi-Scale Exposure Fusion using Median and Recursive Filters Algorithm.

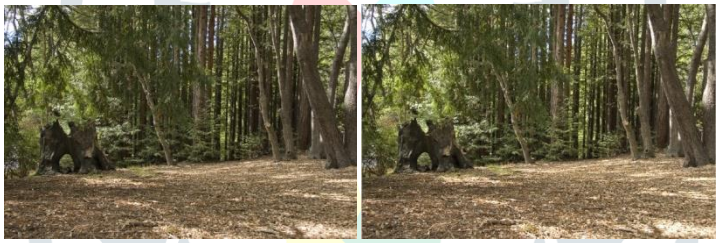

Figure 9: FMMR of Forrest Sequence without and with contrast enhancement

Figure 10 shows the processed images of Tree Scenary by using varied brightness for a series of seven images and a simple Exposure based Fusion Algorithm (which doesn't require any contrast enhancement of images).

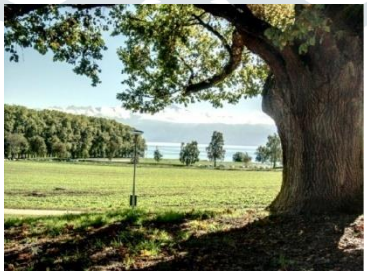

Figure 10: Exposure Fusion of Tree Scenary

Figure 11 shows the processed images of Garage by using varied brightness for a series of six images and a simple Exposure based Fusion Algorithm.

Figure 11: Exposure Fusion of Garage

Figure 12 shows the processed images of Forest Sequence by using varied brightness for a series of four images and a simple Exposure based Fusion Algorithm

Figure 12: Exposure Fusion of Forrest Sequence

Table 1 shows the comparison results of Multi-Scale Exposure of different images without and with Contrast Enhancement. The Algorithm is evaluated by using the parameters like Entropy and Standard Deviation.

As the details show that the images with contrast enhancement yield good value of the parameters, the Multi-Scale Exposure Algorithm when used with contrast enhancement yields better images for human perception.

Table 1: Comparative Results of Multi-Scale Exposure

Designs	Entropy	Standard Deviation
Tree Scenary Without Contrast Enhancement	6.4773	0.7037
Tree Scenary With Contrast Enhancement	6.5433	0.7977
Garage Without Contrast Enhancement	7.1730	0.2625
Garage With Contrast Enhancement	7.2355	0.2975
Forrest Sequence Without Contrast Enhancement	6.7475	0.1485
Forrest Sequence With Contrast Enhancement	6.9182	0.1683

Table 2 shows the comparison results of Fast Multi-Scale Exposure Fusion using Median and Recursive Filters Algorithm for different images without and with Contrast Enhancement for the parameters like Entropy and Standard Deviation.

As the details show that the images with contrast enhancement yield good value of the parameters, the FMMR Algorithm when used with contrast enhancement yields better images for human perception.

Table 2: Comparative Results of FMMR

Designs	Entropy	Standard Deviation
Tree Scenary Without Contrast Enhancement	7.6091	0.2447
Tree Scenary With Contrast Enhancement	7.6729	0.2773
Garage Without Contrast Enhancement	7.6030	0.2283
Garage With Contrast Enhancement	7.5516	0.2518
Forrest Sequence Without Contrast Enhancement	7.4911	0.1948
Forrest Sequence With Contrast Enhancement	7.5991	0.2209

Table 3 shows the comparison results of existing and proposed Multi-Scale Exposure Fusion algorithms for different images without and with Contrast Enhancement for the parameters like Entropy and Standard Deviation. As the details show that the images with FMMR or Exposure fusion yield better values of the parameters than the existing Multi-Scale Exposure Fusion Algorithm.

Table 3: Comparative Results of Existing and Proposed Algorithms

Designs	Entropy	Standard Deviation
FMMR		
Tree Scenary	7.6729	0.2773
Garage	7.5516	0.2518
Forrest Sequence	7.5991	0.2209
MULTI-SCALE EXPOSURE		
Tree Scenary	6.5433	0.7977
Garage	7.2355	0.2975
Forrest sequence	6.9182	0.1683

EXPOSURE FUSION		
Tree Scenary	7.6300	0.3354
Garage	7.5791	0.2610
Forrest sequence	7.6647	0.2113

V. CONCLUSION

The Multi-scale exposure fusion is an effective image enhancement technique for a high dynamic range (HDR) scene with varying lighting conditions. In this project, a new multi-scale exposure fusion algorithm is proposed to merge differently exposed low dynamic range (LDR) images by using the weighted guided image filter (WGIF) to smooth the Gaussian pyramids of weight maps for all the LDR images. The details in the brightest and darkest regions of the HDR scene are preserved better by the proposed algorithm without any relative brightness change in the fused image. In addition, a new weighted structure tensor is introduced to the differently exposed images and it is adopted to design a detail extraction component for the proposed fusion algorithm such that users are allowed to manipulate fine details in the enhanced image according to their preference. The proposed multi-scale exposure fusion algorithm with filter is also applied to design a simple single image brightening algorithm for both low-light imaging and back-light imaging. The proposed design yields better images for human perception. The results are compared for various parameters and the proposed design is found to be a better choice of processing the Multi-Scale Exposure images fusion due to better parameter values of standard deviation and entropy of algorithm.

REFERENCES

[1] Madhu, G. C., Venkatesh, U. S., Diwan, S. P., Chavan, H. P., Saravanakumar, C., & Sakhare, D. T. (2022). Issues and challenges of brain tumor segmentation methods using MRI images. International Journal of Health Sciences, 6(S2), 14793–14805. https://doi.org/10.53730/ijhs.v6nS2.8934.

[2] Vijaya Kishore, V., Kalpana, V. (2020). ROI Segmentation and Detection of Neoplasm Based on Morphology Using Segmentation Operators. In: Hitendra Sarma, T., Sankar, V., Shaik, R. (eds) Emerging Trends in Electrical, Communications, and Information Technologies. Lecture Notes in Electrical Engineering, vol 569. Springer, Singapore. https://doi.org/10.1007/978-981-13-8942-9_41.

[3] Praveena, K., Venkatesh, U. S., Sahoo, N. K., Ramanan, S. V., Bee, M. K. M., & Darwante, N. K. (2022). Brain tumor detection using ANFIS classifier and segmentation. International Journal of Health Sciences, 6(S3), 11817–11828.

[4] Kalpana, V., Vijaya Kishore, V., Praveena, K. (2020). A Common Framework for the Extraction of ILD Patterns from CT Image. In: Hitendra Sarma, T., Sankar, V., Shaik, R. (eds) Emerging Trends in Electrical, Communications, and Information Technologies. Lecture Notes in Electrical Engineering, vol 569. Springer, Singapore. https://doi.org/10.1007/978-981-13-8942-9_42

[5] Vijaya Kishore, V., Kalpana, V. (2020). Effect of Noise on Segmentation Evaluation Parameters. In: Pant, M., Kumar Sharma, T., Arya, R., Sahana, B., Zolfagharinia, H. (eds) Soft Computing: Theories and Applications. Advances in Intelligent Systems and Computing, vol 1154. Springer, Singapore. https://doi.org/10.1007/978-981-15-4032-5_41.

[6] H.D.Praveena, K.Sudha,V.Navya,Ch.V.M.S.Pavan Kumar," High Density Impulse Noise Removal Using Trimmed Global Mean," Journal of Advanced Research in Dynamical and Control Systems, Vol. 9,Sp 14, ISSN:1943-023X, pp:779-788, 2017.

[7] N. Padmaja, A.Anusha, D.V.S Manaswi, & B.Sathish Kumar. (2020). IOT Based Stress Detection and Health Monitoring System. Helix - The Scientific Explorer | Peer Reviewed Bimonthly International Journal, 10(02), 161-167.

[8] Tallapragada, V.V.S., Manga, N.A., Kumar, G.V.P. et al. Mixed image denoising using weighted coding and non-local similarity. SN Appl. Sci. 2, 997 (2020). https://doi.org/10.1007/s42452-020-2816-y.

[9] D.Venkat Reddy, V. V. Satyanarayana Tallapragada*, K. Raghu, M. Venkat Naresh, "Hybrid Tone Mapping with Structural and Edge-preserving Priors", IJAST, vol. 29, no. 7, pp. 5135-5143, Jun. 2020.

[10] V. Vijaya Kishore, V. Kalpana. Application tool for assisting diagnosis and forecast progression of abnormality and medical conditionof patients. Cardiometry; Issue 22; May 2022; p. 520-526; DOI:10.18137/cardiometry.2022.22.520526.

[11] H.D.Praveena, K.Sudha, and P.Geetha, "Support Vector Machine Based Melanoma Skin Cancer Detection," Journal of University of Shanghai for Science and Technology, Vol. 22, Issue 11, pp.1075-1081, Nov 2020.

[12] Tallapragada, V.V.S., Alivelu Manga, N., Nagabhushanam, M.V., Venkatanaresh, M. (2022). Greek Handwritten Character Recognition Using Inception V3. In: Somani, A.K., Mundra, A., Doss, R., Bhattacharya, S. (eds) Smart Systems: Innovations in Computing. Smart Innovation, Systems and Technologies, vol 235. Springer, Singapore. https://doi.org/10.1007/978-981-16-2877-1_23.

[13] Ashreetha, B., Devi, M. R., Kumar, U. P., Mani, M. K., Sahu, D. N., & Reddy, P. C. S. (2022). Soft optimization techniques for automatic liver cancer detection in abdominal liver images. International Journal of Health Sciences, 6(S1).

[14] Dr.M.Dhrani, (2022). Influence of Artificial Intelligence technology slow learners "International journal of early childhood special education (INT-JECSE) ISSN: 1308-5581 Vol 14, Issue 04 2022. DOI: 10.9756/INTJECSE/V1414.233, pp-1824-1829.

[15] H.D.Praveena, Nirmala S. Guptha, Afsaneh Kazemzadeh, B. D. Parameshachari, K. L. Hemalatha, "Effective CBMIR System Using Hybrid Features-Based Independent Condensed Nearest Neighbor Model," Journal of Healthcare Engineering, Vol. 2022, pp.1-9, March 2022.

[16] A. K. N, B. R. Bhatt, P. Anitha, A. K. Yadav, K. K. Devi and V. C. Joshi, "A new Diagnosis using a Parkinson's Disease XGBoost and CNN-based classification model Using ML Techniques," 2022 International Conference on Advanced Computing Technologies and Applications (ICACTA), 2022, pp. 1-6, doi: 10.1109/ICACTA54488.2022.9752867.

[17] Kumar, A. N., Vanaja, D. S., Reddy, A. M., Das, S., Dey, S., & Sucharitha, Y. (2022). Analysis of patient health condition based on hybrid machine learning algorithm. International Journal of Health Sciences, 6(S3), 10532–10544. https://doi.org/10.53730/ijhs.v6nS3.8358

[18] Neelima K, Satyam, Neeruganti Vikram Teja, Dr. N. Gireesh, "Classification of Diabetic Retinopathy Fundus Images using Deep Neural Network," International Conference on "Futuristic Technologies in Control Systems & Renewable Energy" (ICFCR 2022), MES College of Engineering under IEEE Kerala Section, 21-22 July 2022.

[19] S. Q. Wu, Z. G. Li, J. H. Zheng, and Z. J. Zhu, "Exposure robust method for aligning differently exposed images," IEEE Signal Processing Letter, vol. 21, no. 7, pp. 885-889, Jul. 2014.

[20] P. Sen, N. Khademi Kalantari, M. Yaesoubi, S. Darabi, D. Goldman, and E. Shechtman, "Robust patch-based HDR reconstruction of dynamic scenes," ACM Trans. on Graphics, vol. 31, no. 6, Art. 203, Nov. 2012.

[21] J. H. Zheng, Z. G. Li, Z. J. Zhu, S. Q. Wu, and S. Rahardja, "Hybrid patching for a sequence of differently exposed images with moving objects," IEEE Trans. on Image Processing, vol. 22, no. 12, pp.5190- 5201, Dec. 2013.

[22] Z. G. Li, J. H. Zheng, Z. J. Zhu, and S. Q. Wu, "Selectively detail enhanced fusion of differently exposed images with moving objects," IEEE Trans. on Image Processing, vol. 23, no. 10, pp. 4372-4382, Oct. 2014.

[23] Z. G. Li and J. H. Zheng, "Visual salience based tone mapping for high dynamic range images," IEEE Trans. on Industrial Electronics, vol. 61, no. 12, pp. 7076-7082, Dec. 2014.

[24] F. Kou, W. H. Chen, C. Y. Wen, and Z. G. Li, "Gradient domain guided image filtering," IEEE Trans. on Image Processing, vol. 24, no. 11, pp.4528-4539, Nov. 2015.

[25] W. Zhang and W. K. Cham, "Gradient-directed multiexposure composition," IEEE Trans. on Image Processing, vol. 21, no. 4, pp. 2318-2323, Apr. 2012.

[26] S. Li, X. Kang, and J. Hu, "Image fusion with guided filtering," IEEE Trans. Image Processing, vol. 22, no. 7, pp. 2864-2875, Jul. 2013.

[27] M. Song, D. Tao, C. Chen, J. Bu, J. Luo, and C. Zhang, "Probabilistic exposure fusion," IEEE Trans. Image Process., vol. 21, no. 1, pp. 341-357, Jan. 2012.

[28] Z. G. Li, J. H. Zheng, and S. Rahardja, "Detail-enhanced exposure fusion," IEEE Trans. on Image Processing, vol. 21, no 11, pp. 4672-4676, Nov. 2012.

[29] K. Ma, K. Zeng, and Z. Wang, "Perceptual quality assessment for multiexposure image fusion," IEEE Trans. Image Process., vol. 24, no. 11, pp. 3345-3356, Nov. 2015.

[30] Z. G. Li and J. H. Zheng, "Single image brightening via exposure fusion," International Conference on Acoustics, Speech, and Signal Processing, pp. 1756-1760, China, Mar. 2016.